Two-photon optogenetics of neuronal circuits and spines in three dimensions

Adam M. Packer, Darcy S. Peterka, Jan J. Hirtz, Rohit Prakash, Karl Deisseroth and Rafael Yuste

Nature Methods: doi:10.1038/nmeth.2249

Supplementary Figure 1: Spatial resolution of C1V1$_T$ photostimulation.

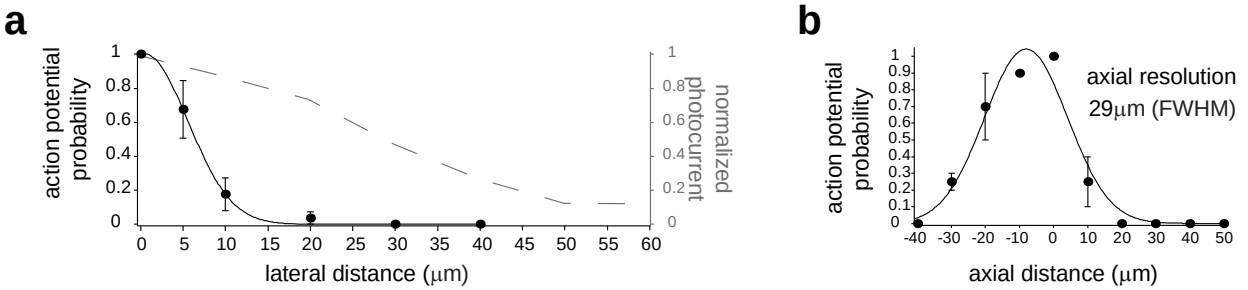

(**a**) Lateral resolution. Action potentials probability after photostimulation of a C1V1$_T$ expressing neuron vs. distance from soma. Somatic-restricted ROI scanning, 20 mW on sample, as described in detail in main text and Methods. APs were produced in individual neurons with a lateral resolution of 6.5 μm. Grey dashed line indicates normalized photocurrent. Even though photocurrents are seen as far out as 50 μm away, the lateral resolution for spiking is significantly higher due to the action potential threshold. It is also likely that small portions of dendrite are in the scanning volume even though the soma is absent, giving rise to small photocurrents. (**b**). Axial resolution. APs were produced in individual neurons with axial resolution of 29.5 μm.

Nature Methods: doi:10.1038/nmeth.2249

Supplementary Figure 2: C1V1$_T$ photostimulation of dendrites result in currents inversely proportional to the distance from the soma.

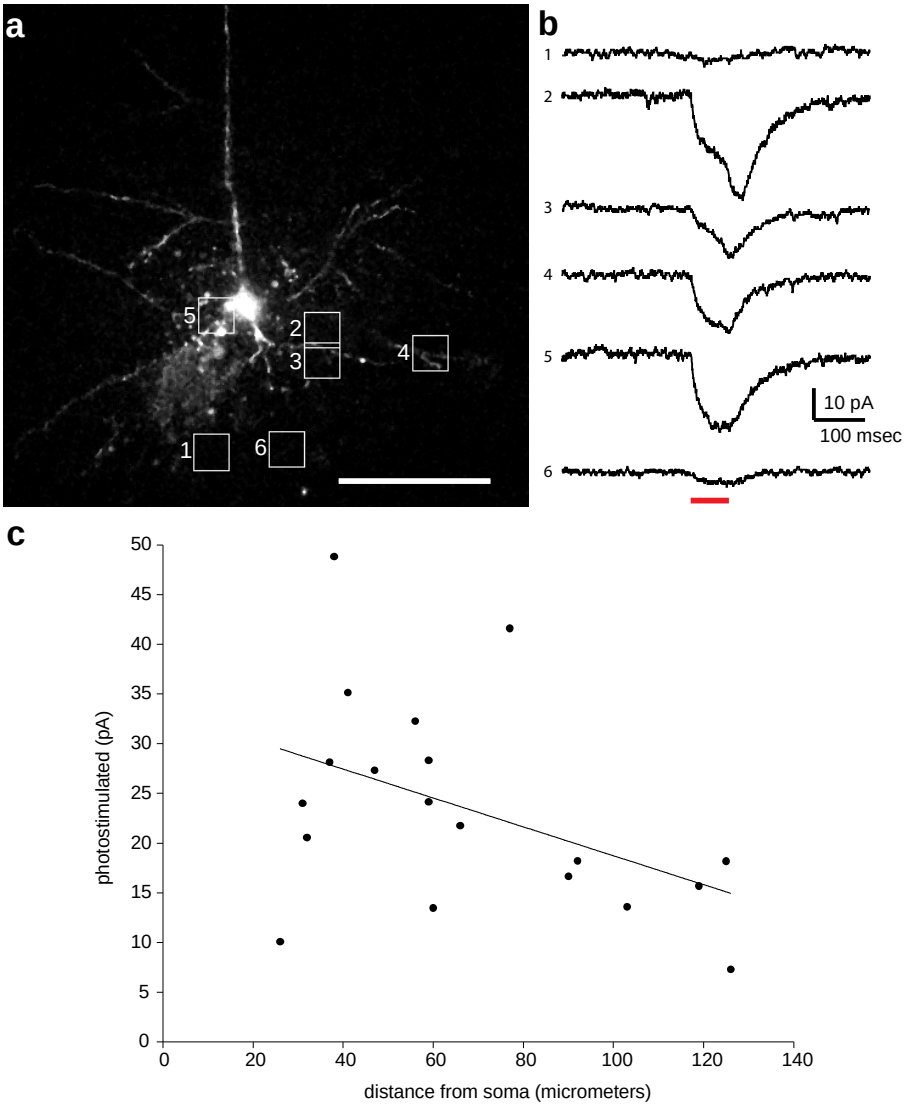

(**a**) A pyramidal cell filled with Alexa 594 imaged with 800 nm excitation. Areas in white boxes were photostimulated via two-photon raster scan (1064 nm, 30 mW on sample). Scale bar, 100 µm. (**b**) Photocurrents elicited during these stimulations. Red bar indicates photostimulation. (**c**). Photostimulated currents decrease with increasing distance to the soma.

Supplementary Figure 3: High resolution of C1V1$_T$ photostimulation on spines and dendrites.

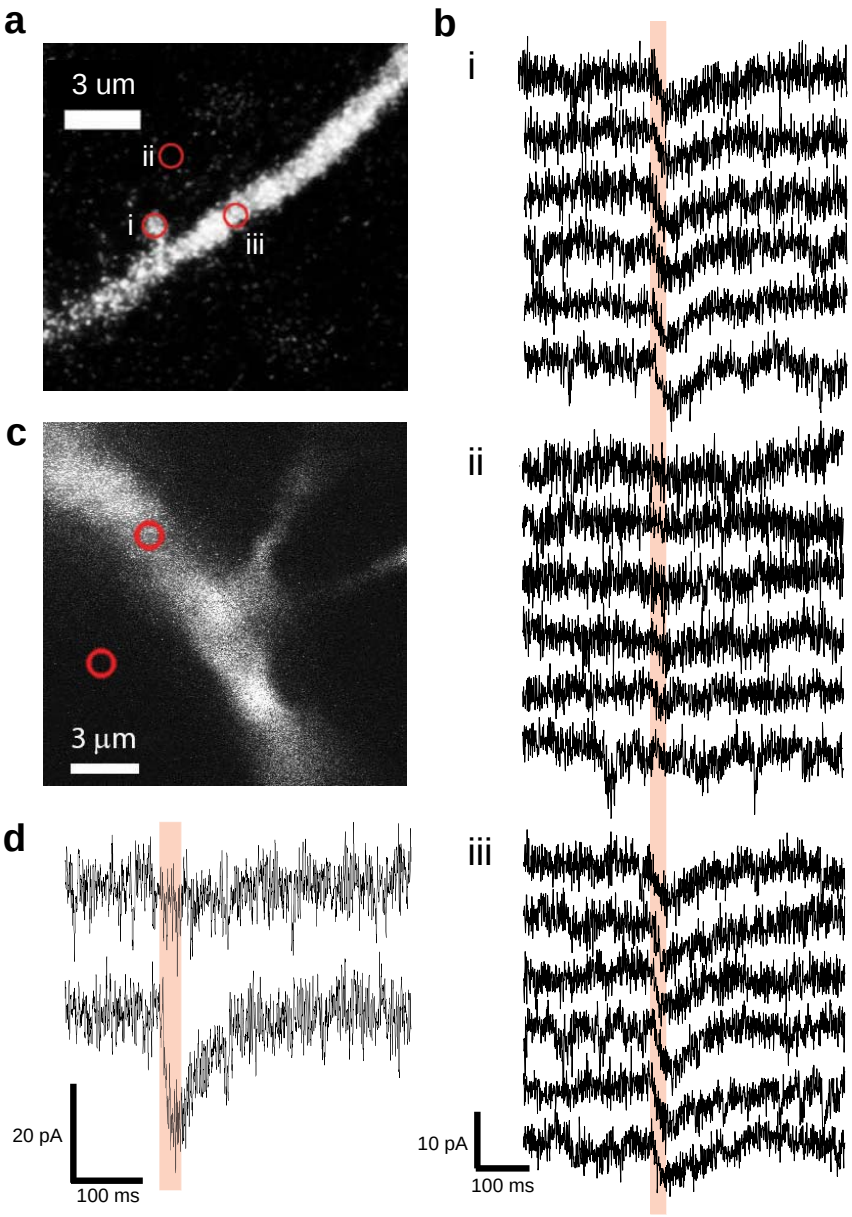

(**a**) Photostimulation target points on a dendritic segments (i: spine, ii: off, iii: dendrite). (**b**) Two-photon elicited photocurrents observed during the stimulation of points in **a**. Individual traces, photostimulation during red bar. Note lack of response of point ii, which is very close to

the spine and dendrite, illustrating the high spatial resolution of the method. (**c**) Target points on a dendrite from a different neuron. (**d**) Average responses from **c** show a strong photocurrent upon photostimulation of the dendrite (red bar), while the point just off the dendrite shows no response. Panel **a** and **c** were imaged with 800 nm for Alexa 594. All photostimulations were performed at 1064 nm with 30 mW on sample.

Nature Methods: doi:10.1038/nmeth.2249

Supplementary Figure 4: Connection searching strategy.

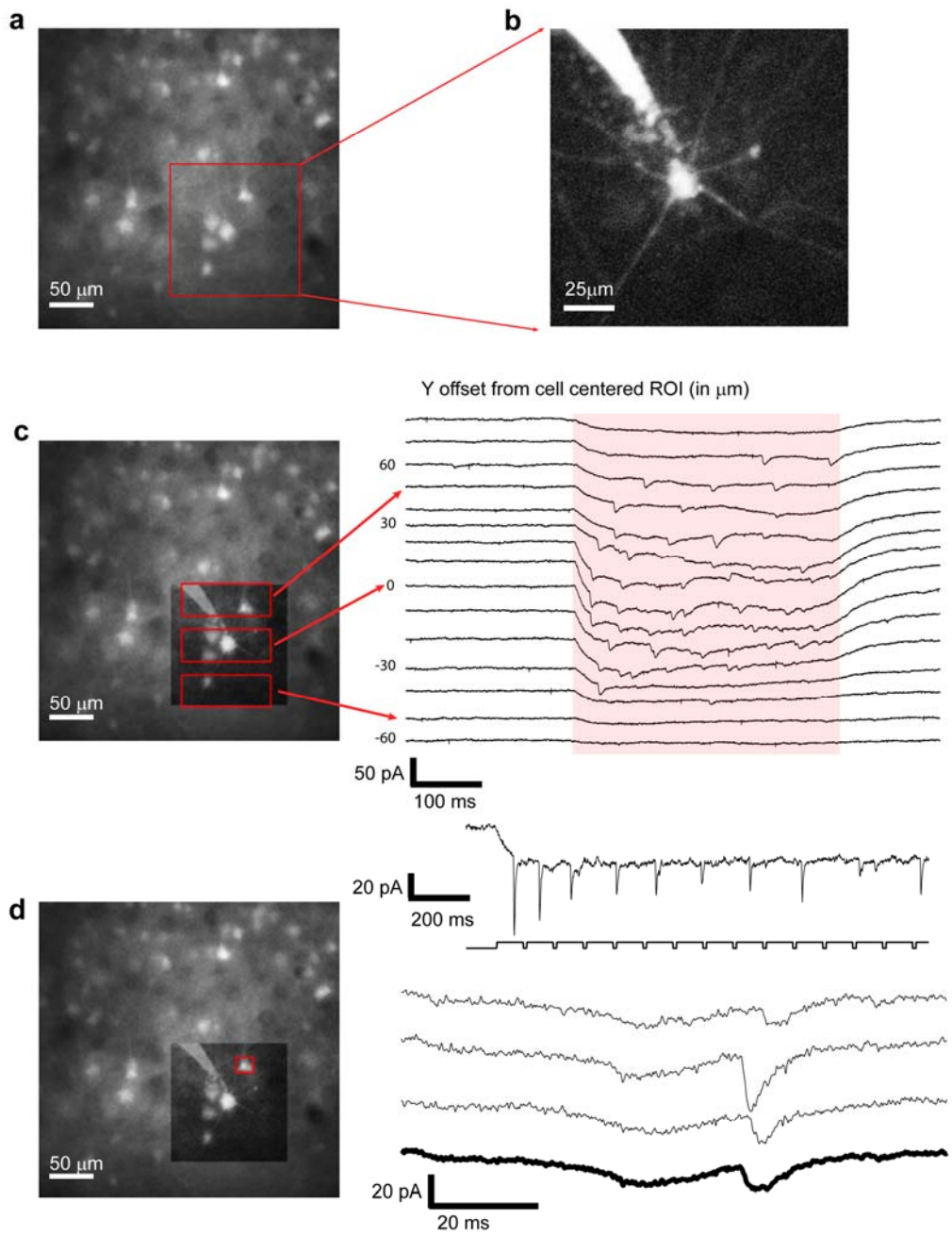

(**a**) A field of neurons with high expression of EYFP/C1V1$_T$ imaged with 940 nm excitation. (**b**) A whole-cell recording from a pyramidal neuron (filled with Alexa 594 and imaged with 800 nm excitation) patched in the area. (**c**) Rectangular areas (red, left) around the recorded

neuron were scanned with the two photon laser (1064 nm, 30 mW on sample) to quickly assess whether any connected neurons resided in the volume. Traces on the right show photocurrents elicited during scans at different vertical spatial offsets from the soma of the recorded neuron (red, photostimulation). Note EPSCs during photostimulations of the ROIs, which contained very nearby, highly expressing, neurons. (**d**) The neuron shown in the red box was selected for more focused photostimulation by directly raster-scanning on its soma. Repeated raster-scanning on the targeted neuron (right, top) showed strong EPSCs time-locked to the photostimulation (black square pulses under trace). Note these raster-scans had a very low interstimulation interval, enabling visualization of both the synaptic depression evident in this connection, and also the increased latency expected from rundown of opsin molecules in the photostimulated neuron as characterized (see **Fig. 1i**). Raster-scans with a larger interstimulation interval (bottom right) show EPSCs with very low jitter, evident in the average response to photostimulation (bold trace).

Nature Methods: doi:10.1038/nmeth.2249

Supplementary Figure 5: Increasing laser intensity during repeated photostimulation enables visualization of a synaptic connection becoming apparent.

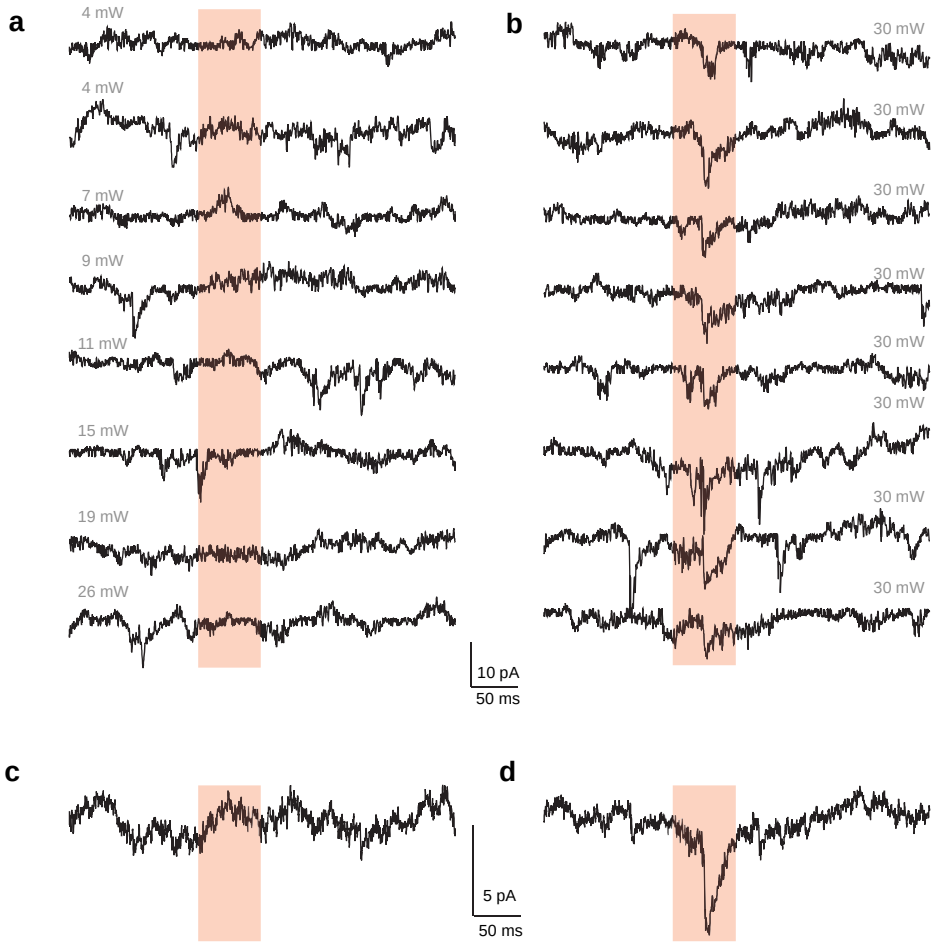

Similar experiment to **Supplementary Fig. 4**. Panel **a** shows traces in a postsynaptic cell while photostimulating a presynaptic neuron at intensities ranging from 4-26 mW (on sample). The presynaptic neuron did not fire an action potential, resulting in no time-locked EPSCs in the individual traces or the average trace (bottom left). Panel **b** shows photostimulation of the same neuron with 30 mW (on sample), at which point the presynaptic neuron fired an action potential at the same time on each scan, resulting in time-locked EPSCs in the individual traces. Panels **c** and **d** show the averages of panels **a** and **b**, respectively. Photostimulation, red bars

Nature Methods: doi:10.1038/nmeth.2249

Supplementary Figure 6: Kinetics of optically detected connections are easily distinguished from direct photostimulation of spines and dendrites.

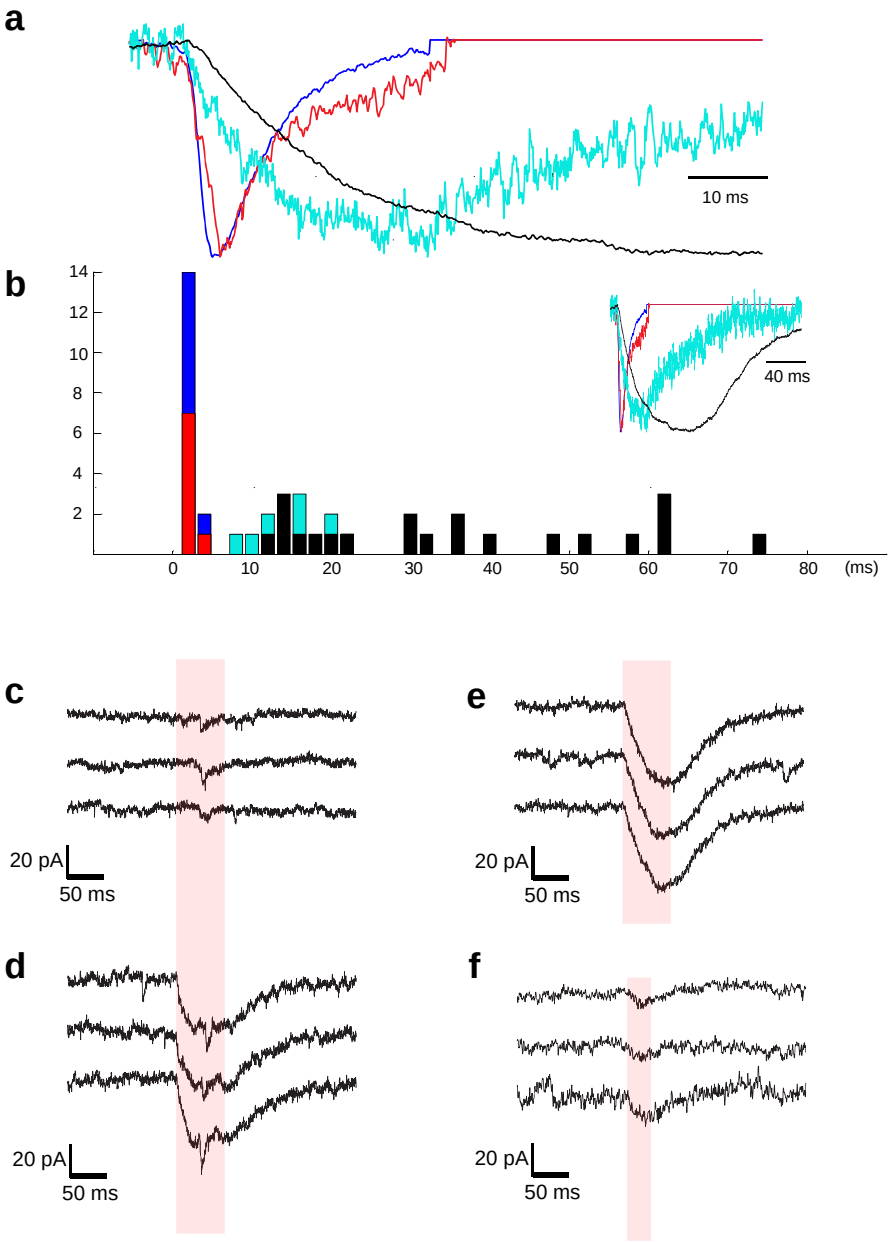

(**a**) Average of the normalized amplitudes of monosynaptic EPSCs recorded from randomly patched pairs of connected cells (blue) is identical to the average of the normalized amplitudes

of monosynaptic EPSCs located via two-photon $C1V1_T$ photostimulation (red). These EPSCs averages are very different to the point photostimulations of spines and dendrites (turquoise) and raster-scan photostimulations of dendritic segments (black). Note also the long fall times (>60 ms) for the direct stimulations, likely dominated by the $C1V1_T$ τ_{off}. (**b**) Histogram of rise times for the EPSCs do not overlap the rise times for photostimulations of spines and dendrites (color code as **a**). (**c**) A connection detected optically, highlighting the time-locked nature of the EPSCs and their fast rise times. (**d**) A connection observed optically riding on top of a direct dendritic stimulation. Note the EPSC is still easily distinguishable due to its fast rise time. (**e**) Direct photostimulation of a dendritic segment is much slower and has larger amplitude than an EPSC (compare to **c**). (**f**) Point photostimulation of a spine/dendrite is also markedly different from the time course of an EPSC. In panels **c-f**, all photostimulations are at 1064 nm with 30 mW on sample.

Nature Methods: doi:10.1038/nmeth.2249

Supplementary Figure 7: Electrophysiological confirmation of a connected pair found optically.

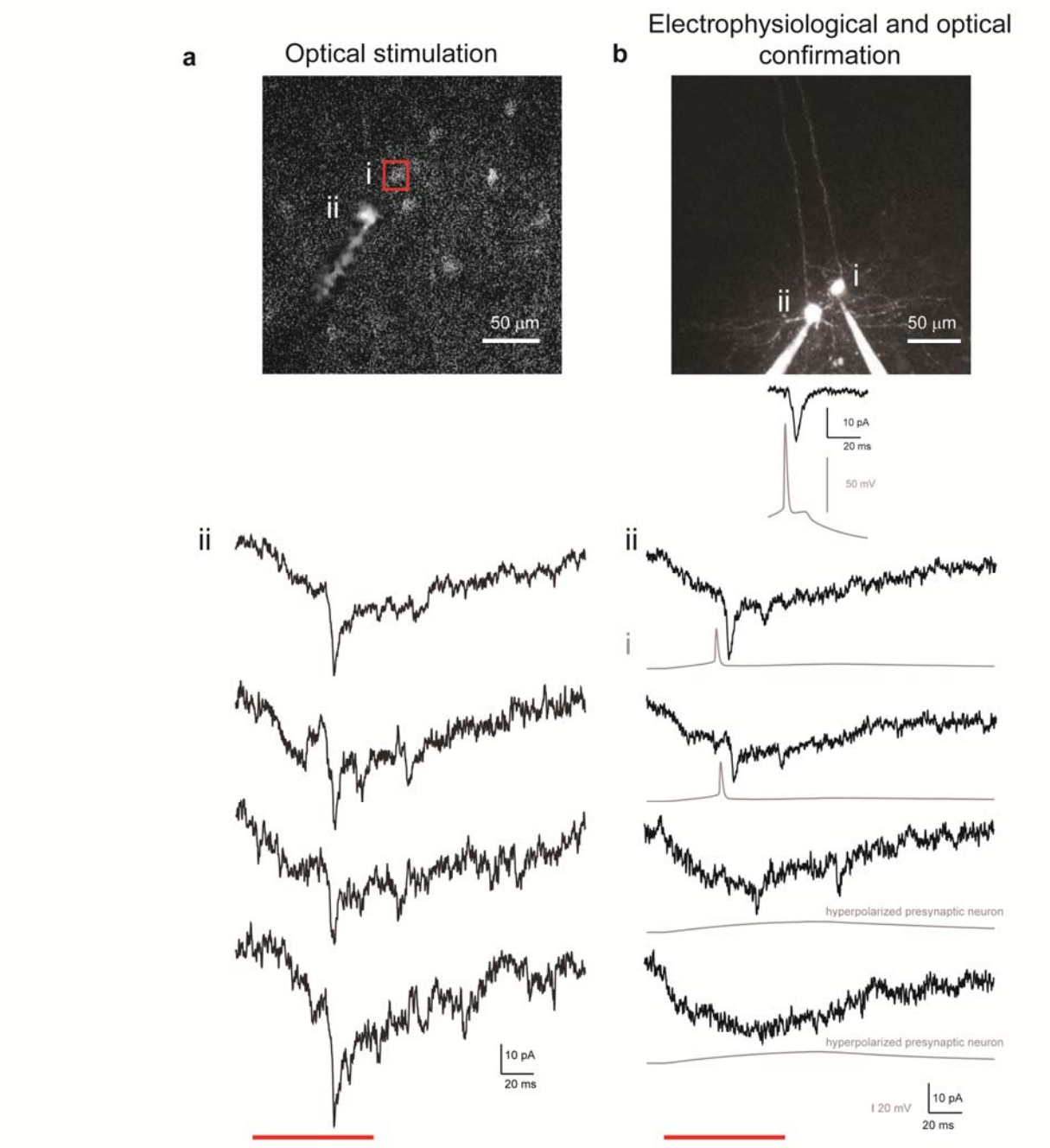

(a) A whole cell recording was made from neuron ii (image, upper left) while neuron i was photostimulated (traces, lower left, photostimulation indicated by red horizontal bar). Note the time-locked EPSCs during every trace. (**b**) A whole-cell recording was made from neuron i

(image, upper right) confirming the connection electrophysiologically (presynaptic action potentials in gray, postsynaptic currents in black). Neuron i was then photostimulated again, resulting in reliable action potentials in neuron i and the same response with time-locked EPSCs in neuron ii. Neuron i was then hyperpolarized during photostimulation, blocking it from producing action potentials, and the time-locked EPSCs in neuron ii disappeared. Panel **a** was imaged with 800nm and 940 nm for Alexa 594 and EYFP, respectively. Panel **b** is imaged at 800nm for Alexa 594. All photostimulations were performed at 1064 nm with 30 mW on sample.

Nature Methods: doi:10.1038/nmeth.2249

Supplementary Figure 8: Measuring synaptic properties with photostimulation.

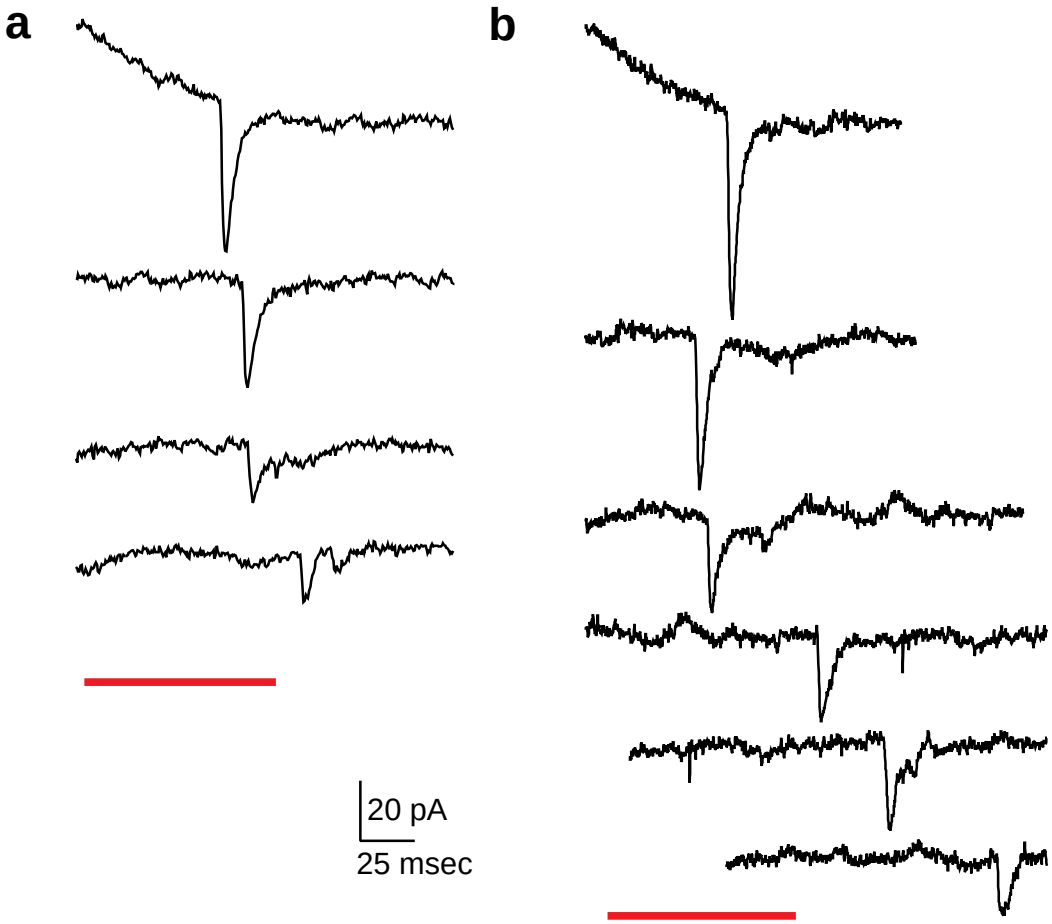

(**a**) Photostimulation of an optically confirmed presynaptic neuron with an inter-photostimulation interval of only 12 milliseconds enabled visualization of the synaptic depression evident in this excitatory connection (PPR=0.70). (**b**) Same as **a** for a different optically confirmed connection (PPR=0.66). Note the increasing latency in the EPSC in both **a** and **b** is due to the increasing latency in the photostimulated action potential in the presynaptic neuron due to the opsin rundown effect shown in **Fig. 1i**.

Nature Methods: doi:10.1038/nmeth.2249

Supplementary Figure 9: SLM calibration and focusing.

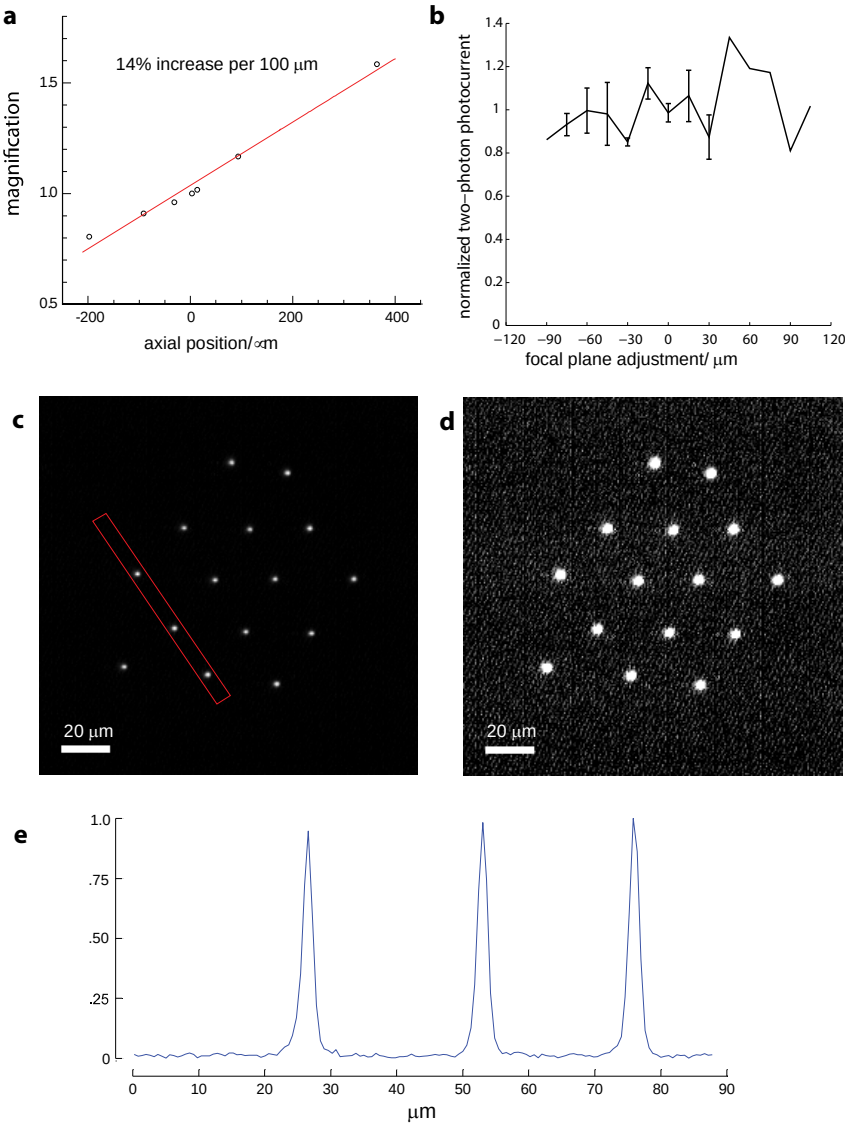

(**a**) Magnification changes linearly with axial distance from the focal plane set by the objective and can be easily calibrated. (**b**) The SLM lens phase was changed while adjusting the focal plane of the microscope (by moving the objective up or down) to maintain the cell body of the scanned neuron in focus. The normalized two-photon current remained the same during these experiments, implying there is no degradation in the scanning efficiency across just over ± 100 μm. (**c**) Widefield emCCD image of Rhodamine 6G (50 μM in methanol) filled thin rectangular

capillary targeted by exact 15 spot pattern that was used to stimulate action potentials in the patched cell that was illuminated by a single one of these beamlets. The high localization and uniformity are apparent. The red rectangle indicates the region whose intensity projection is displayed in **e**. (**d**) Same as in **c**, with higher contrast. The patterned noise on the EMCCD is clearly present, yet it is clear that there is no significant excitation, or spurious intensity outside the beamlets themselves. (**e**) Summed projection of the red ROI shown in **c** highlighting the clear separation and high uniformity of the individual beamlets. For **c**-**e**, the laser power used was matched to approximate the near saturation conditions that we estimate for $C1V1_T$ under our experimental conditions (assume ~250 GM peak for $C1V1_T$, based on ChR2).

Nature Methods: doi:10.1038/nmeth.2249

Supplementary Figure 10: Addressability.

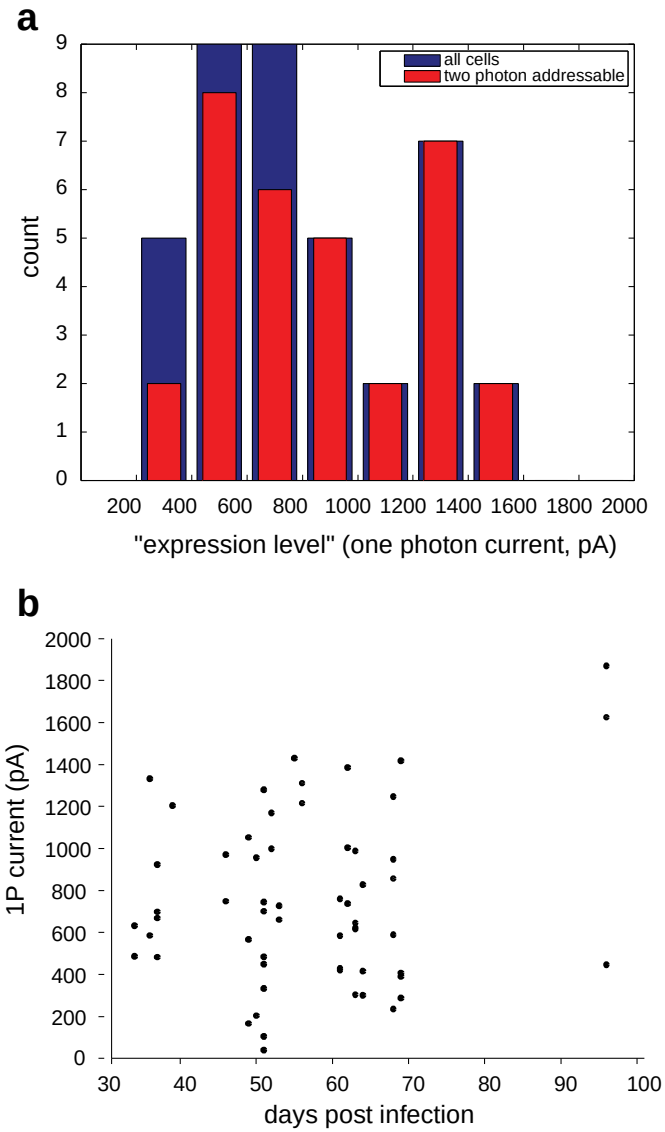

(**a**) Histogram of one photon-currents of all cells where two-photon activation was attempted (blue bars), overlaid with the number of cells that were successfully activated (red bars). A large fraction of low-photocurrent cells were successfully activated, some even quite strongly, with all cells with currents greater than 800 pA addressable. (**b**) The expression level showed no clear trend versus the number of days post-infection (R^2=0.04 for linear fit).

Supplementary Table 1: Pooled data for connections, point photostimulation of dendrites and spines, and photostimulation of dendritic segments.

	EPSCs from patched pairs	Optically confirmed inputs	Point Scan Spines	Point Scan Dendrites	ROI Scans Dendrites
N (targets)	16	8	8	4	21
Trials	351	73	51	31	299
Rise (ms)	2.17	2.3	15.5	15.6	35.8
Std_Rise (ms)	.69	1.1	4.16	5.73	19.4
Range Rise (ms)	1.3-3.8	1.8-3.1	9-22	12-20	13-73
Amp (pA)	17.5	15.6	7.1	6.0	23.3
Std_Amp (pA)	12.8	12.7	1.58	1.14	10.15
Range Amp (pA)	7.3-55	4.5-41	4.9-9	4.0-7.1	10.1-48.8
Delay after illumination (ms)	NA	54.1	<3	<3	<3
Std Delay (ms)	NA	18.6	<1	<1	<2